materials

MDPI

*Supplementary*

# Elucidating the Photocatalytic Behavior of $TiO_2$-$SnS_2$ Composites Based on Their Energy Band Structure

**Marin Kovacic, Jozefina Katic, Hrvoje Kusic *, Ana Loncaric Bozic, and Mirjana Metikos Hukovic ***

Faculty of Chemical Engineering and Technology, University of Zagreb, Marulicev trg 19, Zagreb 10000, Croatia; mkovacic1@fkit.hr (M.K.); jkatic@fkit.hr (J.K.); abozic@fkit.hr (A.L.B.)

* Correspondence: hkusic@fkit.hr (H.K.); mmetik@fkit.hr (M.M.H.); Tel.: +385-1-4597-123 (H.K.); +385-1-4597-140 (M.M.H.); Fax: +385-1-4597-142 (H.K.); +385-1-4597-139 (M.M.H.)

Received: 29 May 2018; Accepted: 14 June 2018; Published: 19 June 2018

**Table S1.** FFD matrix for removal (M1) and conversion (M2) of diclofenac by solar/$TiO_2$-$SnS_2$-COMM process after 60 min exposure.

| Exp. # | Variables | | Experimental results | | Response, $Y$ | |
|---|---|---|---|---|---|---|
| | $X_1$ | $X_3$ | ΔDCF, % | | $Y_1$ | $Y_2$ |
| | coded | coded | removal | conversion | ΔDCF, % removal | ΔDCF, % conversion |
| 1 | -1 | -1 | 68.68 | 53.89 | 72.61 | 57.63 |
| 2 | 0 | -1 | 12.89 | 11.27 | 6.84 | 5.41 |
| 3 | 1 | -1 | 2.01 | 1.36 | 4.14 | 3.47 |
| 4 | -1 | 0 | 80.98 | 66.06 | 78.06 | 63.40 |
| 5 | 0 | 0 | 6.42 | 5.34 | 8.68 | 7.40 |
| 6 | 1 | 0 | 1.71 | 1.07 | 2.38 | 1.67 |
| 7 | -1 | 1 | 82.18 | 68.10 | 81.17 | 67.02 |
| 8 | 0 | 1 | 4.39 | 3.44 | 8.19 | 7.24 |
| 9 | 1 | 1 | 1.07 | 0.44 | -1.73 | -2.27 |

**Table S2.** BBD matrix for removal (M3) and conversion (M4) of diclofenac by solar/$TiO_2$-$SnS_2$-COMM/$H_2O_2$ process after 60 min exposure.

| Exp. # | Variables | | | Experimental results | | Response, $Y$ | |
|---|---|---|---|---|---|---|---|
| | $X_1$ | $X_2$ | $X_3$ | ΔDCF, % | | $Y_1$ | $Y_2$ |
| | coded | coded | coded | removal | conversion | ΔDCF, % removal | ΔDCF, % conversion |
| 1 | -1 | -1 | 0 | 79.41 | 68.04 | 77.37 | 64.93 |
| 2 | 1 | -1 | 0 | 1.80 | 1.17 | 5.26 | 6.50 |
| 3 | -1 | 1 | 0 | 90.11 | 85.78 | 86.65 | 80.44 |
| 4 | 1 | 1 | 0 | 3.19 | 2.93 | 5.23 | 6.05 |
| 5 | -1 | 0 | -1 | 71.99 | 56.34 | 76.50 | 63.47 |
| 6 | 1 | 0 | -1 | 5.13 | 4.92 | 4.14 | 3.61 |
| 7 | -1 | 0 | 1 | 78.05 | 66.77 | 79.04 | 68.08 |
| 8 | 1 | 0 | 1 | 2.37 | 2.26 | -2.13 | -4.87 |
| 9 | 0 | -1 | -1 | 11.45 | 11.27 | 8.98 | 7.25 |
| 10 | 0 | 1 | -1 | 15.56 | 15.31 | 14.52 | 13.51 |
| 11 | 0 | -1 | 1 | 6.99 | 2.24 | 8.03 | 4.04 |
| 12 | 0 | 1 | 1 | 9.27 | 8.82 | 11.74 | 12.84 |
| 13 | 0 | 0 | 0 | 6.64 | 4.55 | 6.65 | 4.55 |
| 14 | 0 | 0 | 0 | 6.64 | 4.52 | 6.65 | 4.55 |
| 15 | 0 | 0 | 0 | 6.66 | 4.58 | 6.65 | 4.55 |

**Table S3.** FFD matrix for removal (M4) and conversion (M5) of diclofenac by solar/$TiO_2$-$SnS_2$-HT process after 60 min exposure.

| Exp. # | Variables | | Experimental results | | Response, $Y$ | |
|---|---|---|---|---|---|---|
| | $X_1$ | $X_3$ | ΔDCF, % | | $Y_1$ | $Y_2$ |
| | coded | coded | removal | conversion | ΔDCF, % removal | ΔDCF, % conversion |
| 1 | -1 | -1 | 71.78 | 58.26 | 69.18 | 58.85 |
| 2 | 0 | -1 | 48.04 | 45.00 | 54.95 | 45.73 |
| 3 | 1 | -1 | 9.98 | 8.33 | 5.67 | 7.01 |
| 4 | -1 | 0 | 88.04 | 75.35 | 87.79 | 73.56 |
| 5 | 0 | 0 | 73.47 | 57.70 | 70.56 | 57.44 |
| 6 | 1 | 0 | 15.11 | 13.67 | 18.28 | 15.71 |
| 7 | -1 | 1 | 89.71 | 76.21 | 92.56 | 77.41 |
| 8 | 0 | 1 | 76.32 | 58.76 | 72.33 | 58.28 |
| 9 | 1 | 1 | 15.93 | 14.27 | 17.07 | 13.55 |

**Table S4.** BBD matrix for removal (M7) and conversion (M8) of diclofenac by solar/$TiO_2$-$SnS_2$-HT/$H_2O_2$ process after 60 min exposure.

| Exp. # | Variables | | | Experimental results | | Response, $Y$ | |
|---|---|---|---|---|---|---|---|
| | $X_1$ | $X_2$ | $X_3$ | ΔDCF, % | | $Y_1$ | $Y_2$ |
| | coded | coded | coded | removal | conversion | ΔDCF, % removal | ΔDCF, % conversion |
| 1 | -1 | -1 | 0 | 91.50 | 82.29 | 95.15 | 79.54 |
| 2 | 1 | -1 | 0 | 10.73 | 7.94 | 8.15 | 7.30 |
| 3 | -1 | 1 | 0 | 94.57 | 91.02 | 97.15 | 91.66 |
| 4 | 1 | 1 | 0 | 41.40 | 16.52 | 37.74 | 19.27 |
| 5 | -1 | 0 | -1 | 89.40 | 69.85 | 84.86 | 70.07 |
| 6 | 1 | 0 | -1 | 12.82 | 7.57 | 14.51 | 5.68 |
| 7 | -1 | 0 | 1 | 91.02 | 79.89 | 89.33 | 81.78 |
| 8 | 1 | 0 | 1 | 8.73 | 1.77 | 13.27 | 1.54 |
| 9 | 0 | -1 | -1 | 37.53 | 24.54 | 38.42 | 27.07 |
| 10 | 0 | 1 | -1 | 50.98 | 41.23 | 52.94 | 40.36 |
| 11 | 0 | -1 | 1 | 40.73 | 31.23 | 38.77 | 32.10 |
| 12 | 0 | 1 | 1 | 56.71 | 45.43 | 55.82 | 42.90 |
| 13 | 0 | 0 | 0 | 53.33 | 39.38 | 53.47 | 39.70 |
| 14 | 0 | 0 | 0 | 53.32 | 39.44 | 53.47 | 39.70 |
| 15 | 0 | 0 | 0 | 53.77 | 40.28 | 53.47 | 39.70 |

**Table S5.** Specific surface area of constituents of studied $TiO_2$-$SnS_2$ composites.

| Material | BET surface area, $m^2\ g^{-1}$ |
|---|---|
| $TiO_2$ P25 | 50 ± 15 [1] |
| $SnS_2$ MKN-900 | 0.83 ± 0.01 |
| $TiO_2$-HT | 128.39 ± 1.87 |
| $SnS_2$-HT | 22.62 ± 0.29 |

**Table S6.** Model equations of derived RSM models for DCF removal and conversion by solar/$TiO_2$-$SnS_2$ without and with an oxidant $H_2O_2$.

| Process | Catalyst type | Model # | Model equation |
|---|---|---|---|
| solar/$TiO_2$-$SnS_2$ | COMM | M1 | $Y_1 = 8.68 - 37.84 \times X_1 + 31.54 \times X_1^2 + 0.68 \times X_3 - 1.17 \times X_3^2 - 3.61 \times X_1 \times X_3$ |

| | | | |
|---|---|---|---|
| solar/$TiO_2$-$SnS_2$/$H_2O_2$ | COMM | M2 | $Y_2 = 7.40 - 30.86 \times X_1 + 25.14 \times X_1^2 + 0.91 \times X_3 - 1.07 \times X_3^2 - 3.78 \times X_1 \times X_3$ |
| | | M3 | $Y_3 = 6.65 - 38.38 \times X_1 + 32.78 \times X_1^2 + 2.31 \times X_2 + 4.21 \times X_2^2 - 0.93 \times X_3 - 0.037 \times X_3^2 - 2.33 \times X_1 \times X_2 - 2.20 \times X_1 \times X_3 - 0.46 \times X_2 \times X_3$ |
| | | M4 | $Y_4 = 4.55 - 33.20 \times X_1 + 29.05 \times X_1^2 + 3.76 \times X_2 + 5.88 \times X_2^2 - 0.97 \times X_3 - 1.02 \times X_3^2 - 3.99 \times X_1 \times X_2 - 3.27 \times X_1 \times X_3 + 0.64 \times X_2 \times X_3$ |
| solar/$TiO_2$-$SnS_2$ | HT | M5 | $Y_5 = 70.56 - 34.75 \times X_1 - 17.52 \times X_1^2 + 8.69 \times X_3 - 6.91 \times X_3^2 - 3.00 \times X_1 \times X_3$ |
| | | M6 | $Y_6 = 57.44 - 28.93 \times X_1 - 12.80 \times X_1^2 + 6.27 \times X_3 - 5.43 \times X_3^2 - 3.00 \times X_1 \times X_3$ |
| solar/$TiO_2$-$SnS_2$/$H_2O_2$ | HT | M7 | $Y_7 = 53.47 - 36.60 \times X_1 + 5.04 \times X_1^2 + 7.90 \times X_2 + 1.03 \times X_2^2 + 0.81 \times X_3 - 8.02 \times X_3^2 + 6.90 \times X_1 \times X_2 - 1.43 \times X_1 \times X_3 + 0.63 \times X_2 \times X_3$ |
| | | M8 | $Y_8 = 39.70 - 36.16 \times X_1 + 6.95 \times X_1^2 + 6.02 \times X_2 + 2.79 \times X_2^2 + 1.89 \times X_3 - 6.88 \times X_3^2 - 0.036 \times X_1 \times X_2 - 3.96 \times X_1 \times X_3 - 0.62 \times X_2 \times X_3$ |

**Table S7.** Analysis of variance (ANOVA) of RSM models M1 and M2 predicting removal and conversion of diclofenac by solar/$TiO_2$-$SnS_2$-COMM process after 60 min exposure (transformed and non-transformed response values).

| **With non-transformed values** | | | | | | | | | | |
|---|---|---|---|---|---|---|---|---|---|---|
| | **Statistical analysis** | | | | | | | | | |
| **Factor (coded)** | **SS** | | **df** | | **MSS** | | ***F*** | | ***p*** | |
| | **M1** | **M2** | **M1** | **M2** | **M1** | **M2** | **M1** | **M2** | **M1** | **M2** |
| Model | 10638.661 | 7044.065 | 5 | 5 | 2127.732 | 1408.813 | 67.919 | 48.417 | 0.0028* | 0.0045* |
| $X_1$ | 8591.707 | 5715.815 | 1 | 1 | 8591.707 | 5715.815 | 274.255 | 196.438 | 0.0005* | 0.0008* |
| $X_1^2$ | 2.737 | 1263.719 | 1 | 1 | 2.737 | 1263.719 | 0.087 | 43.431 | 0.7868 | 0.0071* |
| $X_2$ | 52.105 | 4.977 | 1 | 1 | 52.105 | 4.977 | 1.663 | 0.171 | 0.2876 | 0.7070 |
| $X_2^2$ | 1989.379 | 2.297 | 1 | 1 | 1989.379 | 2.297 | 63.503 | 0.079 | 0.0041* | 0.7970 |
| $X_1 \times X_2$ | 2.732 | 57.258 | 1 | 1 | 2.732 | 57.258 | 0.087 | 1.968 | 0.7870 | 0.2553 |
| Residual | 93.982 | 87.292 | 3 | 3 | 31.327 | 29.097 | | | | |
| Total | 10732.643 | 7131.357 | 8 | 8 | | | | | | |
| **With transformed values** | | | | | | | | | | |
| | **Statistical analysis** | | | | | | | | | |
| **Factor (coded)** | **SS** | | **df** | | **MSS** | | ***F*** | | ***p*** | |
| | **M1** | **M2** | **M1** | **M2** | **M1** | **M2** | **M1** | **M2** | **M1** | **M2** |
| Model | 0.796 | 28.833 | 5 | 5 | 0.159 | 5.767 | 103.142 | 67.386 | 0.0015* | 0.0028* |
| $X_1$ | 0.731 | 27.534 | 1 | 1 | 0.731 | 27.534 | 473.293 | 321.747 | 0.0002* | 0.0004* |
| $X_1^2$ | 0.013 | 0.091 | 1 | 1 | 0.013 | 0.091 | 8.181 | 1.059 | 0.0646 | 0.3791 |
| $X_2$ | 0.034 | 0.725 | 1 | 1 | 0.034 | 0.725 | 21.817 | 8.478 | 0.0185* | 0.0619 |
| $X_2^2$ | 0.001 | 0.015 | 1 | 1 | 0.001 | 0.015 | 0.505 | 0.172 | 0.5287 | 0.7058 |
| $X_1 \times X_2$ | 0.018 | 0.469 | 1 | 1 | 0.018 | 0.469 | 11.915 | 5.476 | 0.0409* | 0.1012 |
| Residual | 0.005 | 0.257 | 3 | 3 | 0.002 | 0.086 | | | | |
| Total | 0.801 | 29.090 | 8 | 8 | | | | | | |

*$p$<0.05 means that model or model term is significant

**Table S8.** Analysis of variance (ANOVA) of RSM models M3 and M4 predicting removal and conversion of diclofenac by solar/$TiO_2$-$SnS_2$-COMM/$H_2O_2$ process after 60 min exposure (transformed and non-transformed response values).

| **With non-transformed values** | | | | | | | | | | |
|---|---|---|---|---|---|---|---|---|---|---|
| **Factor (coded)** | **Statistical analysis** | | | | | | | | | |
| | **SS** | | **df** | | **MSS** | | ***F*** | | ***p*** | |
| | **M3** | **M4** | **M3** | **M4** | **M3** | **M4** | **M3** | **M4** | **M3** | **M4** |
| Model | 15881.136 | 12260.441 | 9 | 9 | 1764.571 | 1362.271 | 98.879 | 30.899 | <0.0001* | 0.0007* |
| $X_1$ | 11785.644 | 8820.169 | 1 | 1 | 11785.644 | 8820.169 | 660.420 | 200.058 | <0.0001* | <0.0001* |
| $X_1^2$ | 3966.537 | 3115.435 | 1 | 1 | 3966.537 | 3115.435 | 222.269 | 70.664 | <0.0001* | 0.0004* |
| $X_2$ | 42.769 | 113.390 | 1 | 1 | 42.769 | 113.390 | 2.397 | 2.572 | 0.1823 | 0.1697 |
| $X_2^2$ | 65.323 | 127.863 | 1 | 1 | 65.323 | 127.863 | 3.660 | 2.900 | 0.1139 | 0.1493 |
| $X_3$ | 6.956 | 7.515 | 1 | 1 | 6.956 | 7.515 | 0.390 | 0.170 | 0.5598 | 0.6968 |
| $X_3^2$ | 0.005 | 3.854 | 1 | 1 | 0.005 | 3.854 | 0.000 | 0.087 | 0.9874 | 0.7794 |
| $X_1 \times X_2$ | 21.655 | 63.776 | 1 | 1 | 21.655 | 63.776 | 1.213 | 1.447 | 0.3208 | 0.2829 |
| $X_1 \times X_3$ | 19.409 | 42.870 | 1 | 1 | 19.409 | 42.870 | 1.088 | 0.972 | 0.3448 | 0.3694 |
| $X_2 \times X_3$ | 0.844 | 1.618 | 1 | 1 | 0.844 | 1.618 | 0.047 | 0.037 | 0.8364 | 0.8556 |
| Residual | 89.228 | 220.440 | 5 | 5 | 17.846 | 44.088 | | | | |
| Total | 15970.365 | 12480.881 | 14 | 14 | | | | | | |
| **With transformed values** | | | | | | | | | | |
| **Factor (coded)** | **Statistical analysis** | | | | | | | | | |
| | **SS** | | **df** | | **MSS** | | ***F*** | | ***p*** | |
| | **M3** | **M4** | **M3** | **M4** | **M3** | **M4** | **M3** | **M4** | **M3** | **M4** |
| Model | 24.376 | 27.235 | 9 | 9 | 2.708 | 3.026 | 98.253 | 22.738 | <0.0001* | 0.0015* |
| $X_1$ | 21.982 | 21.975 | 1 | 1 | 21.982 | 21.975 | 797.443 | 165.123 | <0.0001* | <0.0001* |
| $X_1^2$ | 1.345 | 2.331 | 1 | 1 | 1.345 | 2.331 | 48.806 | 17.514 | 0.0009* | 0.0086* |
| $X_2$ | 0.208 | 0.999 | 1 | 1 | 0.208 | 0.999 | 7.555 | 7.510 | 0.0404* | 0.0408* |
| $X_2^2$ | 0.093 | 0.103 | 1 | 1 | 0.093 | 0.103 | 3.362 | 0.776 | 0.1262 | 0.4188 |
| $X_3$ | 0.362 | 0.963 | 1 | 1 | 0.362 | 0.963 | 13.138 | 7.235 | 0.0151* | 0.0433* |
| $X_3^2$ | 0.302 | 0.456 | 1 | 1 | 0.302 | 0.456 | 10.939 | 3.430 | 0.0213* | 0.1232 |
| $X_1 \times X_2$ | 0.050 | 0.118 | 1 | 1 | 0.050 | 0.118 | 1.821 | 0.888 | 0.2351 | 0.3893 |
| $X_1 \times X_3$ | 0.181 | 0.224 | 1 | 1 | 0.181 | 0.224 | 6.570 | 1.686 | 0.0505 | 0.2508 |
| $X_2 \times X_3$ | 0.000 | 0.283 | 1 | 1 | 0.000 | 0.283 | 0.006 | 2.130 | 0.9433 | 0.2043 |
| Residual | 0.138 | 0.665 | 5 | 5 | 0.028 | 0.133 | | | | |
| Total | 24.513 | 27.901 | 14 | 14 | | | | | | |

**Table S9.** Analysis of variance (ANOVA) of RSM models **M5** and **M6** predicting removal and conversion of diclofenac by solar/$TiO_2$-$SnS_2$-HT process after 60 min exposure.

| **Factor (coded)** | **Statistical analysis** | | | | | | | | | |
|---|---|---|---|---|---|---|---|---|---|---|
| | **SS** | | **df** | | **MSS** | | ***F*** | | ***p*** | |
| | **M5** | **M6** | **M5** | **M6** | **M5** | **M6** | **M5** | **M6** | **M5** | **M6** |
| Model | 8444.841 | 5679.537 | 5 | 5 | 1688.968 | 1135.907 | 43.308 | 279.397 | 0.0054* | 0.0003* |
| $X_1$ | 7245.976 | 5020.347 | 1 | 1 | 7245.976 | 5020.347 | 185.799 | 1234.846 | 0.0009* | <0.0001* |
| $X_1^2$ | 614.018 | 327.830 | 1 | 1 | 614.018 | 327.830 | 15.744 | 80.636 | 0.0286* | 0.0029* |
| $X_2$ | 453.327 | 236.213 | 1 | 1 | 453.327 | 236.213 | 11.624 | 58.101 | 0.0422* | 0.0047* |
| $X_2^2$ | 95.634 | 59.073 | 1 | 1 | 95.634 | 59.073 | 2.452 | 14.530 | 0.2153 | 0.0317* |
| $X_1 \times X_2$ | 35.886 | 36.074 | 1 | 1 | 35.886 | 36.074 | 0.920 | 8.873 | 0.4082 | 0.0587 |
| Residual | 116.997 | 12.197 | 3 | 3 | 38.999 | 4.066 | | | | |
| Total | 8561.837 | 5691.734 | 8 | 8 | | | | | | |

*$p$<0.05 means that model or model term is significant

**Table S10.** Analysis of variance (ANOVA) of RSM models **M7** and **M8** predicting removal and conversion of diclofenac by solar/$TiO_2$-$SnS_2$-HT/$H_2O_2$ process after 60 min exposure .

| Factor (coded) | Statistical analysis | | | | | | | | | |
|---|---|---|---|---|---|---|---|---|---|---|
| | SS | | df | | MSS | | *F* | | *p* | |
| | M7 | M8 | M7 | M8 | M7 | M8 | M7 | M8 | M7 | M8 |
| Model | 11783.882 | 11252.799 | 9 | 9 | 1309.320 | 1250.311 | 67.906 | 164.620 | 0.0001* | <0.0001* |
| $X_1$ | 10717.658 | 10457.913 | 1 | 1 | 10717.66 | 10457.913 | 555.855 | 1376.923 | <0.0001* | <0.0001* |
| $X_1^2$ | 93.846 | 178.300 | 1 | 1 | 93.846 | 178.300 | 4.867 | 23.476 | 0.0785 | 0.0047* |
| $X_2$ | 498.655 | 290.338 | 1 | 1 | 498.655 | 290.338 | 25.862 | 38.227 | 0.0038* | 0.0016* |
| $X_2^2$ | 3.943 | 28.701 | 1 | 1 | 3.943 | 28.701 | 0.205 | 3.779 | 0.6700 | 0.1095 |
| $X_3$ | 5.201 | 28.624 | 1 | 1 | 5.201 | 28.624 | 0.270 | 3.769 | 0.6257 | 0.1099 |
| $X_3^2$ | 237.463 | 174.949 | 1 | 1 | 237.463 | 174.949 | 12.316 | 23.034 | 0.0171* | 0.0049* |
| $X_1 \times X_2$ | 190.432 | 0.005 | 1 | 1 | 190.432 | 0.005 | 9.876 | 0.001 | 0.0256* | 0.9801 |
| $X_1 \times X_3$ | 8.156 | 62.772 | 1 | 1 | 8.156 | 62.772 | 0.423 | 8.265 | 0.5441 | 0.0348* |
| $X_2 \times X_3$ | 1.598 | 1.540 | 1 | 1 | 1.598 | 1.540 | 0.083 | 0.203 | 0.7850 | 0.6714 |
| Residual | 96.407 | 37.976 | 5 | 5 | 19.281 | 7.595 | | | | |
| Total | 11880.289 | 11290.775 | 14 | 14 | | | | | | |

*$p$<0.05 means that model or model term is significant

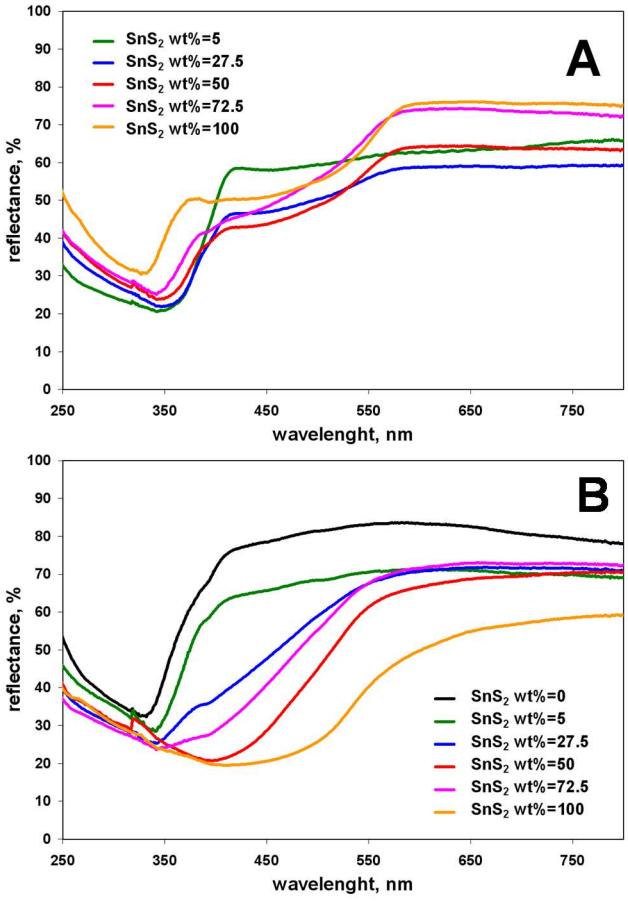


**Figure S1.** Diffuse reflectance spectra of immobilized $TiO_2$-$SnS_2$ composites with different $SnS_2$ wt%; commercial (COMM) (**A**) and hydrothermal (HT) (**B**)

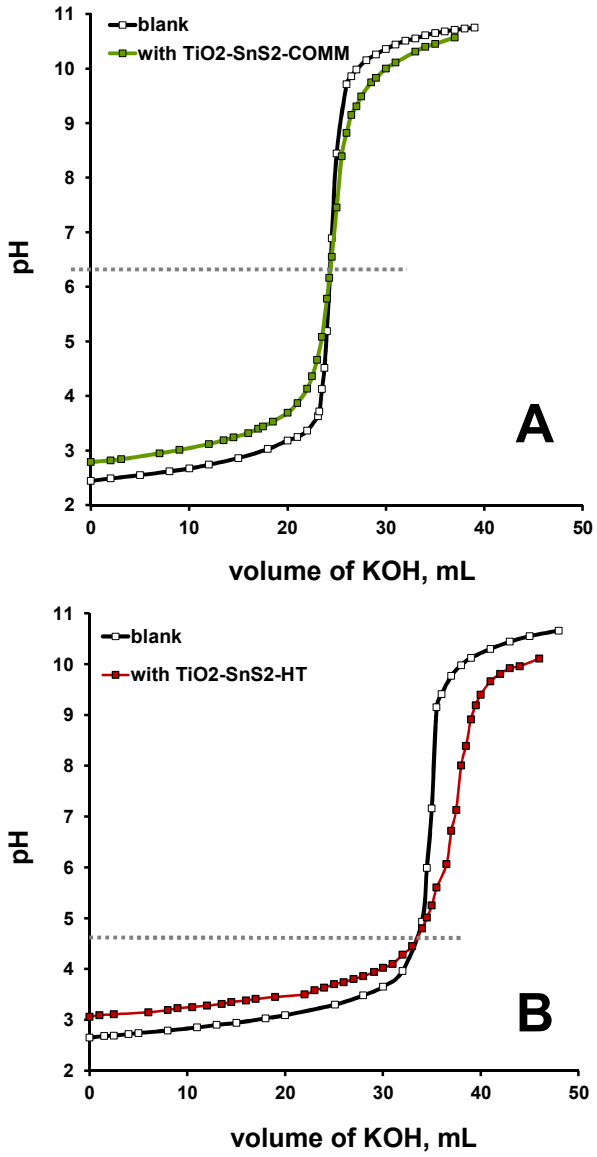


**Figure S2.** Determination of $pH_{PZC}$ values $TiO_2$-$SnS_2$-COMM (**A**) and $TiO_2$-$SnS_2$-HT (**B**) composites.

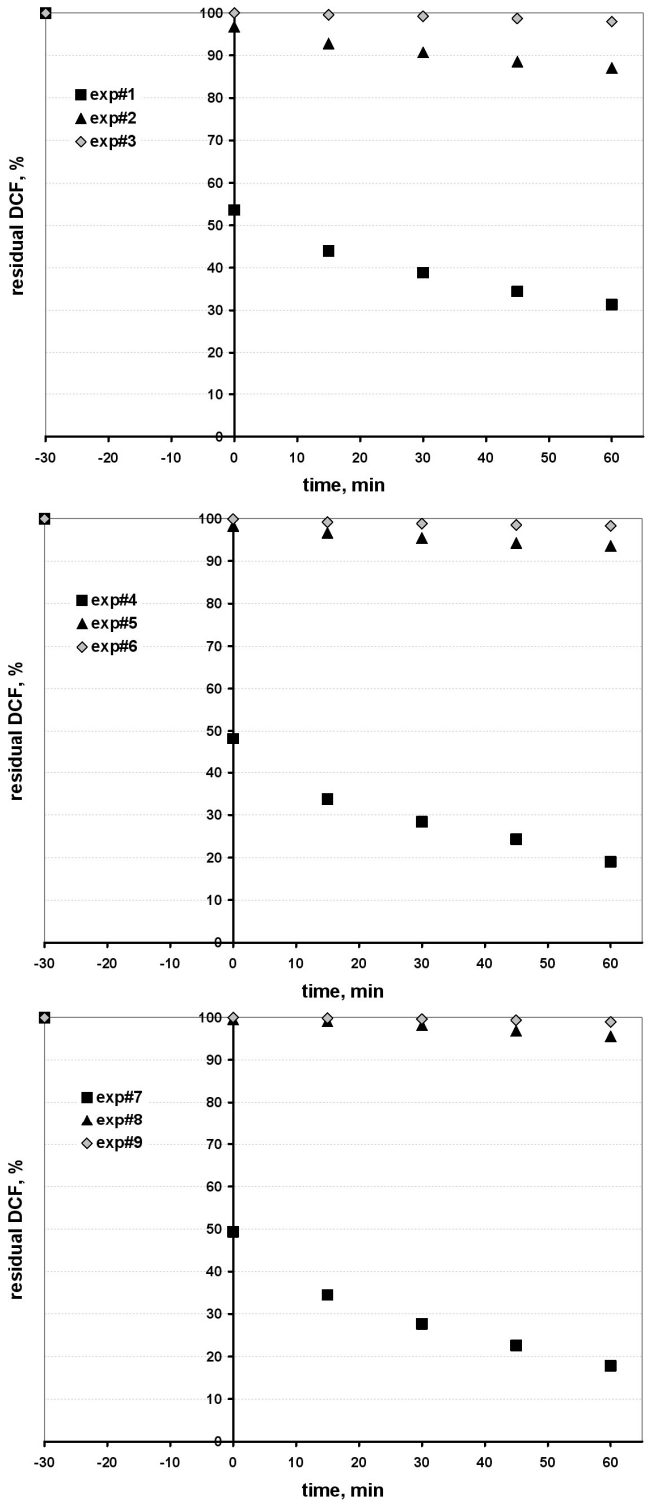


**Figure S3.** Kinetics of DCF removal by solar/$TiO_2$-$SnS_2$-COMM process; $TiO_2$-$SnS_2$-COMM prepared by immobilization using AEROXIDE $TIO_2$ P25 and $SnS_2$ MKN-900 (Experimental conditions listed in Table 1, and experimental matrix provided by FFD, Table S1, Supplementary material).

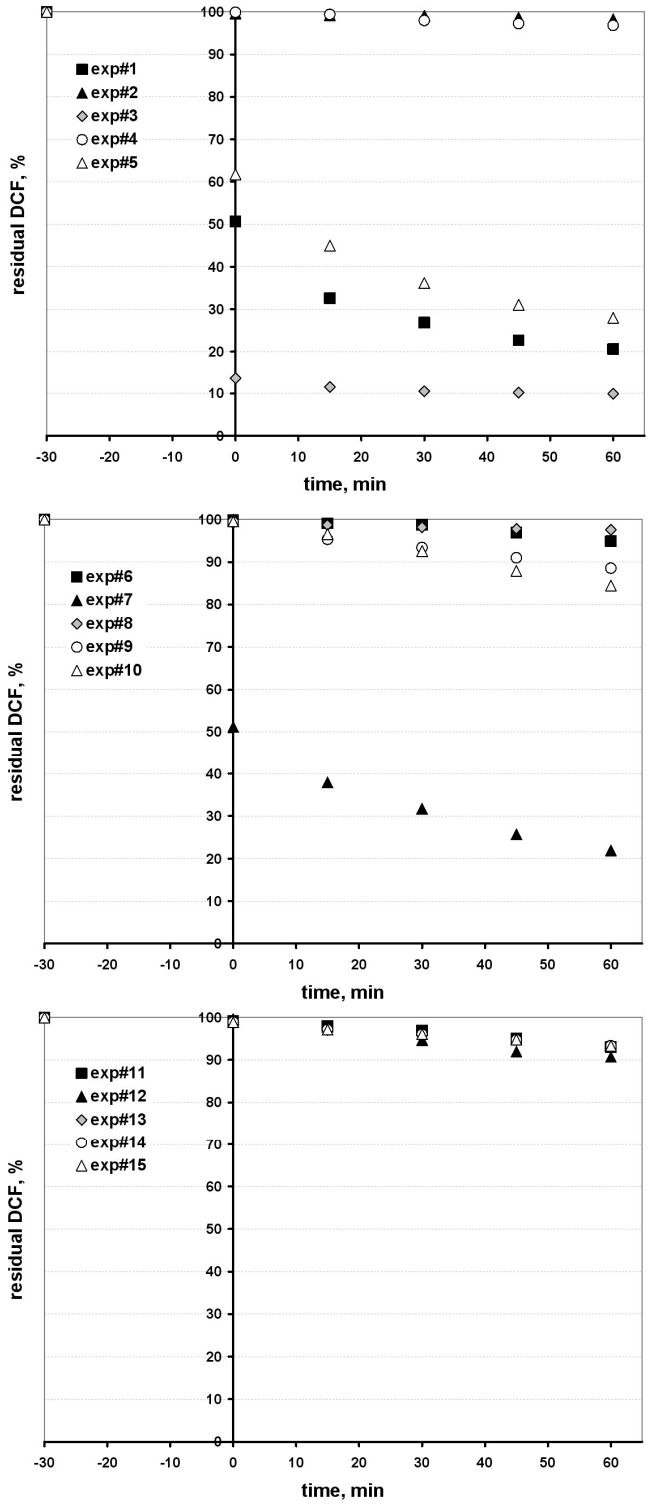


**Figure S4.** Kinetics of DCF removal by solar/$TiO_2$-$SnS_2$-COMM/$H_2O_2$ process; $TiO_2$-$SnS_2$-COMM prepared by immobilization using AEROXIDE $TIO_2$ P25 and $SnS_2$ MKN-900 (Experimental conditions listed in Table 1, and experimental matrix provided by BBD, Table S2, Supplementary material).

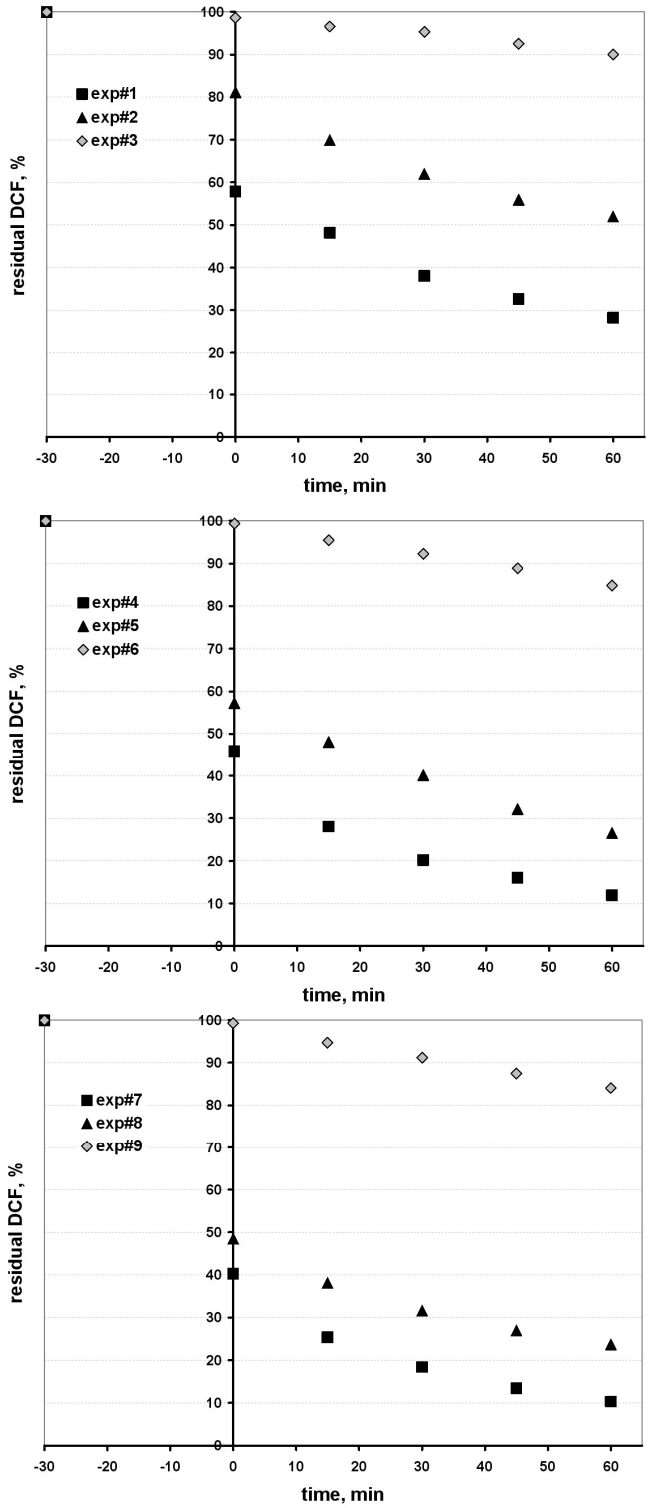


**Figure S5.** Kinetics of DCF removal by solar/$TiO_2$-$SnS_2$-HT process; $TiO_2$-$SnS_2$-HT prepared by hydrothermal method (Experimental conditions listed in Table 1, and experimental matrix provided by FFD, Table S3, Supplementary material).

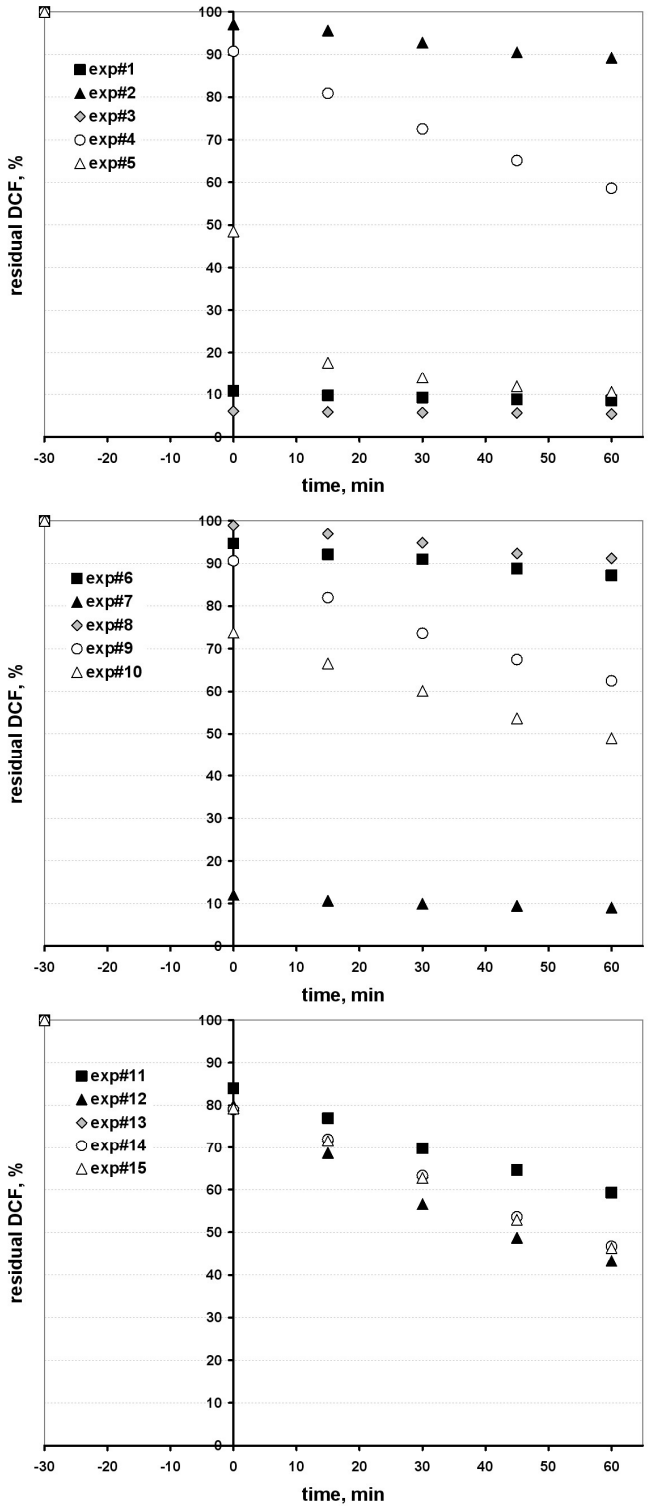


**Figure S6.** Kinetics of DCF removal by solar/$TiO_2$-$SnS_2$-HT/$H_2O_2$ process; $TiO_2$-$SnS_2$-HT prepared by hydrothermal method (Experimental conditions listed in Table 1, and experimental matrix provided by BBD, Table S4, Supplementary material).

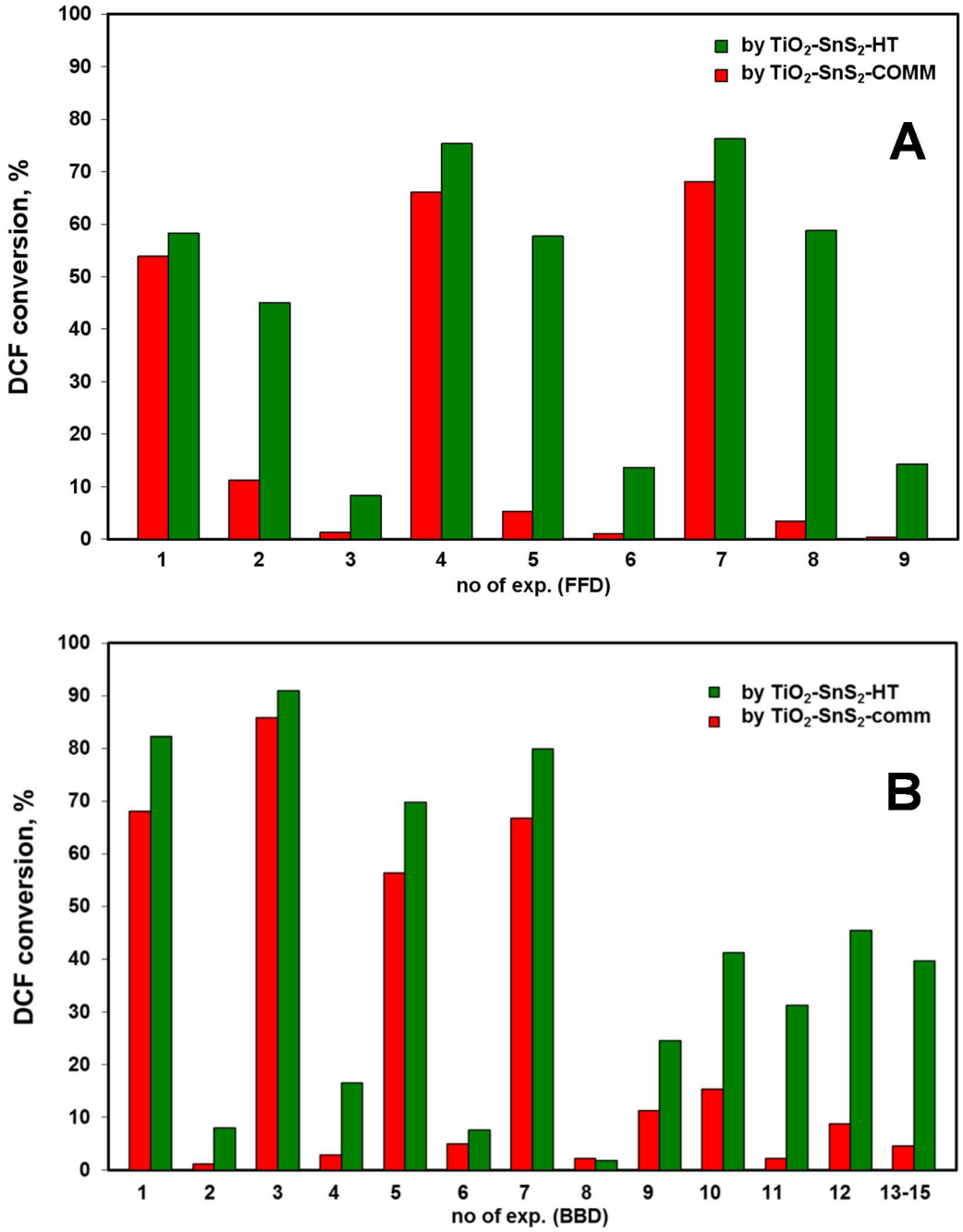


**Figure S7.** Comparison of DCF conversion using $TiO_2$-$SnS_2$-COMM and $TiO_2$-$SnS_2$-HT without $H_2O_2$ (**A**) and with $H_2O_2$ addition (**B**) under solar radiation at conditions set by FFD (Tables 1, and S1 and S3, Supplementary material) and BBD (Tables 1, and S2 and S4, Supplementary material), respectively.

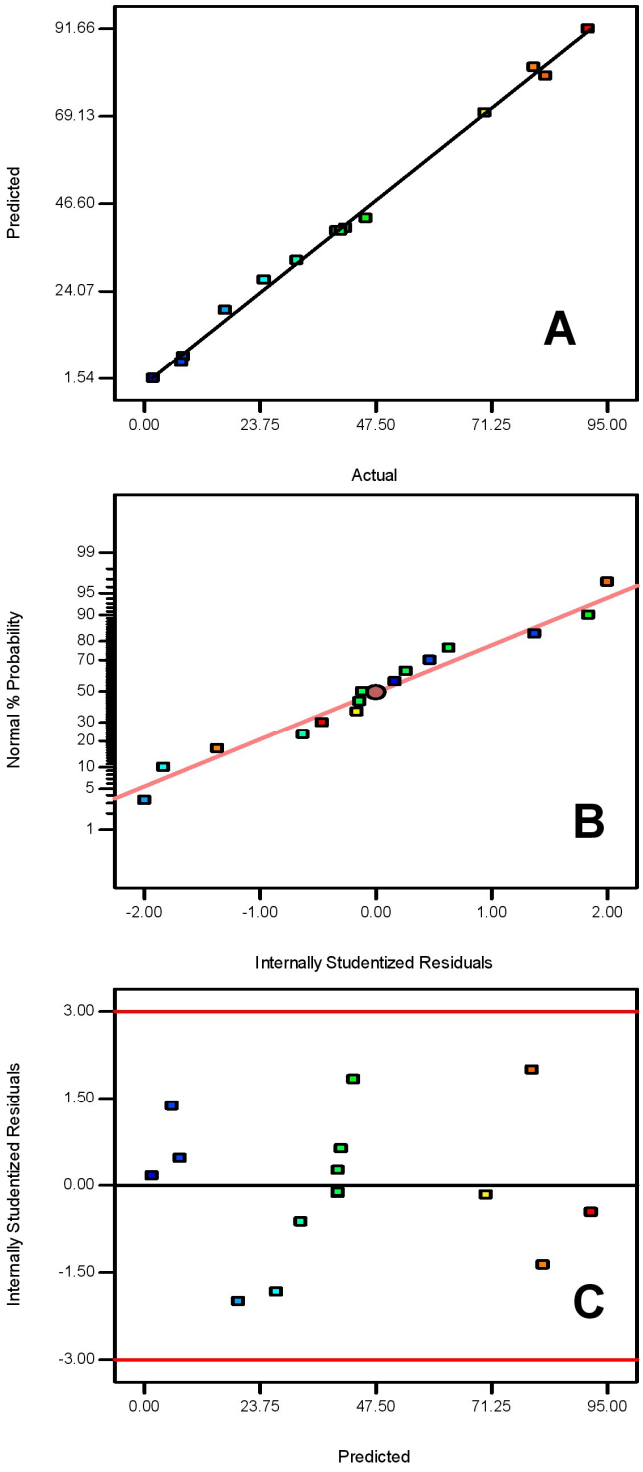


**Figure S8.** Residual diagnostics of model M6 for the prediction of the conversion of DCF by solar/$TiO_2$-$SnS_2$-HT/$H_2O_2$ process: (**A**) observed *vs.* predicted plot, (**B**) normal probability plot, and (**C**) internally studentized residuals *vs.* predicted values plot.

## Detailed Experimental section related to (1) Determination of semiconducting properties by electrochemical measurements, and (2) Calculations and procedure used in RSM modeling

*1. .Determination of semiconducting properties by electrochemical measurements*

Circular shaped titanium samples (Alfa Aesar, 99.9 wt.% Ti) were abraded with 1000 grit SiC papers, ultrasonically cleaned with ethanol and redistilled water and served as solid substrates for $TiO_2$-HT and $SnS_2$-HT pure components, as well as for $TiO_2$-$SnS_2$-COMM and $TiO_2$-$SnS_2$-HT

composites immobilization as was described in the Experimental section, subsection *2.2. Photocatalysts synthesis and immobilization* (main text). As prepared substrates were embedded in a Teflon holder, with an area, $A$=1 cm$^2$ exposed to the solution and were used as working electrodes.

All electrochemical measurements were performed in a conventional three–electrode cell: the working electrode was Ti coated electrode, the counter electrode was a large area platinum electrode and the reference electrode, to which all potentials in the paper are referred, was Ag | AgCl in 3.0 mol dm$^{-3}$ KCl ($E$ = 0.208 V vs. standard hydrogen electrode). The electrolyte was 3% NaCl solution, pure or spiked with DCF (0.1 mM). A Solartron potentiostat/galvanostat 1287 with FRA 1260 controlled by CorrWare® and ZView® softwares was used in these measurements.

The structure of the solid | liquid interface, i.e., the structure of the $TiO_2$-$SnS_2$ catalysts | electrolyte solution interface ($TiO_2$-$SnS_2$-COMM and $TiO_2$-$SnS_2$-HT composite films on titanium substrate) was investigated at the open circuit potential ($E_{ocp}$) using electrochemical impedance spectroscopy (EIS) performed in the frequency range from 100 kHz to 5 mHz at an *ac* voltage amplitude of ±5 mV. The experimental data were fitted using the complex non–linear least squares (CNLS) fit analysis software [2] and values of the elements of the proposed electric equivalent circuit (EEC) were derived with $\chi^2$ values less than $5 \times 10^{-3}$ (errors in parameter values of 1–3%).

Due to the frequency dispersion (mostly attributed to the "capacitance dispersion"), the capacitor in EECs was replaced with the constant phase element (CPE). The impedance of CPE is defined as $Z(\mathrm{CPE})=[Q(j\omega)^n]^{-1}$, where $j\omega$ is the complex variable for sinusoidal perturbations with $\omega=2\pi f$, and $n$ is the exponent of CPE, while $Q$ is the frequency–independent parameter of CPE, which represents a pure capacitance when $n$ = 1 [3]. Values of $0.70 < n < 1$ indicate inhomogeneities at the microscopic level at the metal | electrolyte interface (surface roughness, adsorbed species, etc.) [4,5]. The numerical values of interfacial capacitances, $C$ were calculated using the Brug's relation, valid when the ohmic (electrolyte) resistance, $R_\Omega$ is much smaller than the charge–transfer resistance [3]:

$$C = (Q \cdot R_\Omega^{1-n})^{1/n} \quad (1)$$

The electronic–semiconducting properties of $TiO_2$-HT, $SnS_2$-HT, $TiO_2$-$SnS_2$-COMM and $TiO_2$-$SnS_2$-HT catalyst films were investigated by Mott–Schottky method [6]. The capacitance values of the titanium | composite film | solution interface, required for Mott–Schottky analysis, were obtained from EIS measurements. The imaginary part of impedance ($Z_{imag}$) was recorded as a function of the electrode potential and the frequency (ranging from 3000−30 Hz). The potential was swept in the negative direction from 0 V at a sweep rate of 50 mV s$^{-1}$. The rapid cathodic scan of 50 mV s$^{-1}$ was used to avoid the change in the film thickness during measurements [7]. From the measured $Z_{imag}$ values, it was possible to calculate CPE parameter $Q = -1/\omega\, Z_{imag}$ taking into account the angular frequency, $\omega=2\pi f$. From $Q$ value and CPE exponent $n$ and $R_\Omega$, the effective interfacial capacitance, $C$, was calculated using the expression developed by Brug et al. [3]; eq. (1). The $C$ values consist of the series combination of Helmholtz double layer capacitance ($C_H$) with the parallel combination of the space–charge capacitance ($C_{sc}$) and is equal to:

$$C^{-1} = C_H^{-1} + C_{sc}^{-1} \quad (2)$$

All capacitance values were corrected taking Helmholtz capacitance to be 50 μF cm$^{-2}$ [8].

To avoid the frequency dispersion of the effective interfacial capacitance in MS tests and eliminate the contribution of the surface states, the data obtained at seven frequencies (ranging from 3000−30 Hz) were analyzed according to the procedure proposed by Harrington et al. [8,9]. Detailed description of Devine−Harrington procedure can be found in literature [10–12]. By applying Devine−Harrington procedure, the characteristic frequency was determined to be 1000 Hz. Hence the results provided refer to this frequency.

*2. .Calculations and procedure used in RSM modeling*

The influence of pH, [$H_2O_2$] and $SnS_2$ wt % within $TiO_2$-$SnS_2$ composites, on DCF removal and conversion was correlated by means of response surface modeling (RSM). The values of process parameters are represented by independent variables: $X_1$, $X_2$ and $X_3$ (Table 1, main text), and according to the number of parameters to be varied within solar driven photocatalytic treatment, experimental matrices were expressed by $3^2$ FFD for solar/$TiO_2$-$SnS_2$ (Tables S1 and S3, respectively) and BBD for solar/$TiO_2$-$SnS_2$/$H_2O_2$ processes (Tables S2 and S4, respectively). DCF removal and conversion extents after 60 min exposure to solar irradiation were chosen as processes responses ($Y$). The combined influence of studied parameters on processes performance is described by quadratic polynomial equations, i.e. RSM models [13], and evaluated by the (i) analysis of variance (ANOVA) considering following statistical parameters: Fisher $F$-test value ($F$), its probability value ($p$), regression coefficients (pure; $R^2$, adjusted; $R_{adj}^2$, predicted; $R_{pre}^2$), $t$-test value, and (ii) graphical based analysis, so-called "residual diagnostic" (RD): including normal probability test, Levene's test, and constant variance test. The calculations were performed by STATISTICA 12.7, StatSoft&Dell; and Design-Expert 10.0, StatEase, software packages.

## References


1. Evonik Industries, AEROXIDE®, AERODISP® and AEROPERL® Titanium Dioxide as photocatalyst, Technical information 1243. Available on line: http://www.aerosil.com/sites/lists/RE/DocumentsSI/TI-1243-Titanium-Dioxide-as-Photocatalyst-EN.pdf. (Accessed on May 02, 2018)
2. Boukamp, A. A nonlinear least squares fit procedure for analysis of immittance data of electrochemical systems, Solid State Ion. **1986**, *20*, 31–44.
3. Brug, G.J.; Van der Eeden, A.L.G.; Sluyters-Rehbach, M.; Sluyters, J.H. The analysis of electrode impedances complicated by the presence of a constant phase element. *J. Electroanal. Chem*. 1984, 176 275–295.
4. Jorcin, J.B.; Orazem, M.E.; Pebere, N.; Tribollet, B. CPE analysis by local electrochemical impedance spectroscopy. *Electrochim. Acta* **2006**, *51*, 1473–1479.
5. Lasia, A. Electrochemical Impedance Spectroscopy and its Applications, in *Modern Aspects of Electrochemistry*; Conway, B.E.; Bockris, J.; White, R.E.; Eds.; Kluwer Academic/Plenum Publishers: New York, NY, USA, 1999; Volume 32, p. 143–248.
6. Orazem, M.E.; Tribollet, B. *Electrochemical Impedance Spectroscopy*, John Wiley & Sons: New York, NY, USA, 2008.
7. Harrington, S.P.; Devine, T.M.; Analysis of electrodes displaying frequency dispersion in Mott-Shottky tests. *J. Electrochem. Soc*. **2008**, *155*, C381–C386.
8. Katić, J.; Metikoš-Huković, M.; Šarić, I.; Petravić, M. Semiconducting properties of the oxide films formed on tin: Capacitive and XPS studies. *J. Electrochem. Soc*. **2016**, *163*, C221–C227.
9. Harrington, S.P.; Wang, F.; Devine, T.M. The structure and electronic properties of passive and prepassive films of iron in borate buffer. *Electrochim. Acta* **2010**, *55*, 4092–4102.
10. Katić, J.; Metikoš-Huković, M. Correlation between electronic and corrosion properties of the passive oxide film on Nitinol. *Acta Chim. Slov*. **2014**, *61*, 350–356.
11. Katić, J.; Metikoš-Huković, M.; Milošev, I. Ionic and electronic conductivity of the anodic films on nickel. *J. Electrochem. Soc*. **2015**, *162*, C767–C774.
12. Katić, J.; Metikoš-Huković, M.; Šarić, I.; Petravić, M. Electronic structure and redox behavior of tin sulfide films potentiostatically formed on tin. *J. Electrochem. Soc*. **2017**, *164*, C383–C389.
13. Myers, R.H.; Montgomery, D.C.; Anderson-Cook, C.M. *Response Surface Methodology: Process and Product Optimization Using Designed Experiments*, 3rd ed.; John Wiley & Sons: Hoboken, NJ, USA, 2009.